

000 001 002 003 CALIBRATION OF ORDINAL REGRESSION NETWORKS 004 005 006 007

008 **Anonymous authors**
 009 Paper under double-blind review
 010
 011
 012
 013
 014
 015
 016
 017
 018
 019
 020
 021
 022

023 ABSTRACT 024

025 Recent studies have shown that deep neural networks are not well-calibrated and
 026 produce over-confident predictions. The miscalibration issue primarily stems from
 027 the minimization of cross-entropy, which aims to align predicted softmax prob-
 028 abilities with one-hot labels. In ordinal regression tasks, this problem is com-
 029 pounded by an additional challenge: the expectation that softmax probabilities
 030 should exhibit unimodal distribution is not met with cross-entropy. Rather, the or-
 031 dinal regression literature has focused on unimodality and overlooked calibration.
 032 To address these issues, we propose a novel loss function that introduces order-
 033 aware calibration, ensuring that prediction confidence adheres to ordinal relation-
 034 ships between classes. It incorporates soft ordinal encoding and label-smoothing-
 035 based regularization to enforce both calibration and unimodality. Extensive exper-
 036 iments across three popular ordinal regression benchmarks demonstrate that our
 037 approach achieves state-of-the-art calibration without compromising accuracy.
 038

039 1 INTRODUCTION 040

041 Despite significant advances in ordinal regression tasks, such as medical diagnosis and age estima-
 042 tion, one critical aspect has often been overlooked: calibration. While research has predominantly
 043 focused on improving accuracy, the importance of well-calibrated predictions in ordinal regression
 044 remains underexplored. In high-risk applications, where both accuracy and reliability are crucial,
 045 poorly calibrated models can lead to overconfident or underconfident decisions, potentially resulting
 046 in harmful outcomes.

047 Ordinal regression, also called ordinal classification, involves a natural ordering between class la-
 048 bels, setting it apart from nominal tasks. Approaches such as regression (Fu & Huang, 2008; Pan
 049 et al., 2018; Yang et al., 2018; Li et al., 2019), classification (Liu et al., 2020; Polat et al., 2022b;
 050 Vargas et al., 2022), and ranking-based methods (Niu et al., 2016; Chen et al., 2017; Cao et al.,
 051 2020; Shi et al., 2023) have been developed to capture this ordinal structure, often outperforming
 052 traditional frameworks by better aligning with the data’s inherent order. However, insufficient at-
 053 tention to calibration has led to unreliable confidence estimates, particularly in fields like medical
 054 diagnosis, where the consequences of miscalibration can be severe (Guo et al., 2017).

055 Calibration aims to align a model’s confidence estimates with actual accuracy, ensuring that pre-
 056 dicted probabilities reflect the likelihood of correct predictions. Without proper calibration, models
 057 risk overconfidence, especially when encountering ambiguous or noisy data, which can lead to un-
 058 safe decisions in sensitive domains such as healthcare (Neumann et al., 2018; Moon et al., 2020).
 059 For example, in disease severity prediction, a model should adjust its confidence based on input
 060 uncertainty, particularly in ambiguous cases.

061 In addition to calibration, unimodality is crucial in ordinal classification. Unimodal distributions
 062 ensure that the model assigns the highest probability to the correct label, with probabilities gradu-
 063 ally decreasing as the distance from the true label increases, preventing paradoxical or inconsis-
 064 tent predictions (Li et al., 2022; Vargas et al., 2022).

065 To address these dual challenges of calibration and unimodality, we propose Oridnal Regression
 066 loss for Calibration and Unimodality (ORCU), a novel loss function that integrates order-aware cal-
 067ibration with a unimodal regularization term. Traditional regularization techniques often neglect
 068 the ordered structure of ordinal tasks, but ORCU enforces both calibration and unimodality by ex-
 069 plicitly modeling the ordinal relationships between classes. This ensures well-calibrated confidence
 070 estimates that reflect the full ordinal structure, enabling the model to produce unimodal probabil-

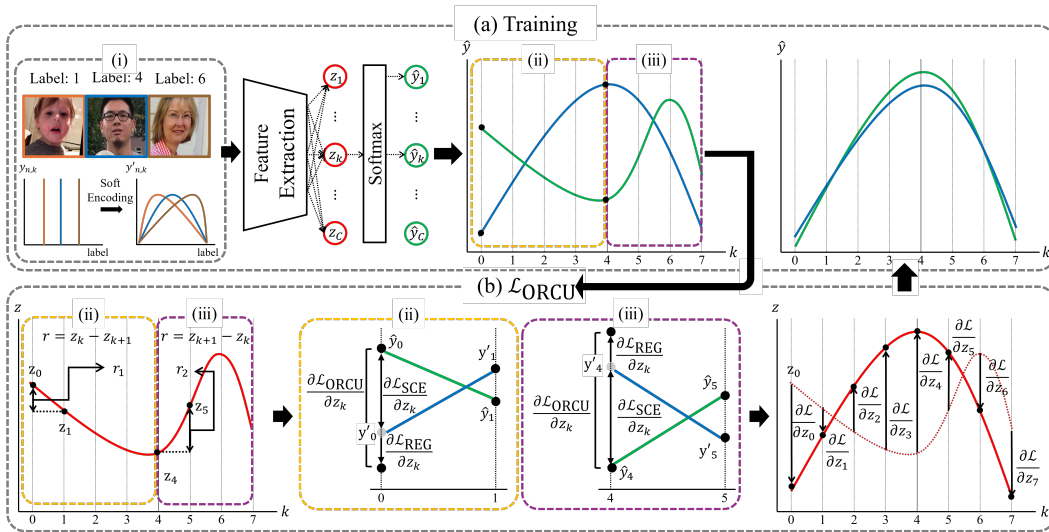


Figure 1: Overview of how the ORCU achieves improved calibration and unimodal probability distribution in ordinal classification. It illustrates the role of the calibration regularization term, \mathcal{L}_{REG} , when applied to soft label encoding for the Adience dataset (8 ordinal classes representing age groups) as an example. Soft encoding is applied to hard ordinal labels (a-i). Then, \mathcal{L}_{REG} is applied differently for $k < y_n$ (a-ii) and $k \geq y_n$ (a-iii). (b) illustrates how $\mathcal{L}_{\text{ORCU}}$'s gradients are computed with examples shown for $k = 0, 4$. See section 3.4 and Table 1 for gradient analysis.

ity distributions that smoothly decrease as the distance from the true label increases. As a result, ORCU not only improves prediction accuracy but also enhances the reliability and trustworthiness of predictions, particularly in high-stakes applications like medical diagnosis.

Contributions We make the following key contributions: (1) We propose ORCU, a novel loss function that unifies calibration and unimodality within a single framework for ordinal regression. ORCU incorporates soft encoding and introduces a regularization term that uniquely applies order-aware conditions, ensuring that predicted probabilities reflect the ordinal relationships between classes while providing reliable confidence estimates. (2) We provide a comprehensive analysis demonstrating how ORCU effectively balances the trade-off between well-calibrated confidence estimates and accurate predictions. By integrating calibration and unimodality constraints into a single loss function, ORCU addresses the limitations of existing methods that focus solely on either calibration or ordinal structure. (3) By unifying calibration and unimodality constraints, we establish a new benchmark for reliable ordinal classification, significantly advancing the state of the art and paving the way for future research on trustworthy models for ordinal tasks.

2 RELATED WORKS

Ordinal Regression Ordinal regression addresses the challenge of predicting a target value with an inherent order, unlike nominal classification, where no ordinal relationships exist between labels. Given an input x , the goal is to predict a label y , which follows an ordinal relationship such that $y_1 \prec y_2 \prec \dots \prec y_C$, with \prec representing a label order (e.g., y_i is less severe or earlier in rank than y_{i+1}). Approaches to ordinal classification are broadly divided into three categories: regression methods, classification-based methods, and ranking-based methods. In regression methods (Fu & Huang, 2008; Pan et al., 2018; Yang et al., 2018; Li et al., 2019), ordinal labels y are treated as continuous variables, applying losses like L1 or L2 to predict a scalar value reflecting the label ordering. Classification-based methods (Liu et al., 2020; Polat et al., 2022b; Vargas et al., 2022) discretize the continuous target space into bins, treating each bin as a class $y \in \{1, 2, \dots, C\}$ and predicting the class directly. Ranking-based methods (Niu et al., 2016; Chen et al., 2017; Cao et al., 2020; Shi et al., 2023) decompose the task into $C - 1$ binary classifiers, each determining whether the true label y exceeds a threshold, capturing the ordinal relationships between labels.

108 **Loss functions for ordinal regression** The inherent limitations of Cross-Entropy (CE) loss in
 109 handling ordinal relationships have led to several modified approaches (see Section 3.1). One such
 110 approach is Soft ORDinal (SORD) encoding method (Diaz & Marathe, 2019), which adjusts the
 111 label distribution by using soft labels to capture the proximity between classes, thereby ensuring
 112 smoother and more order-aware predictions (see Section 3.2). Class Distance Weighted Cross-
 113 Entropy (CDW-CE) (Polat et al., 2022b), on the other hand, keeps the traditional label structure
 114 but incorporates a distance-based penalty into the loss function, encouraging predictions closer to
 115 the true class and better aligned with the ordinal structure. CO2 (Albuquerque et al., 2021) extends
 116 CE with a regularization term enforcing unimodality, ensuring that predicted probabilities decrease
 117 smoothly as the distance from the true label increases. In contrast, Probabilistic Ordinal Embeddings
 118 (POE) (Li et al., 2021) introduces both a regularization term and architectural changes, representing
 119 each label as a probability distribution, thereby modeling both uncertainty and ordinal relationships.
 120

121 **Regularization-based loss functions for calibration** Calibration, which aims to align predicted
 122 confidence with actual accuracy, is particularly critical in high-risk tasks involving ordinal cate-
 123 gories. Several regularization-based approaches have been proposed to improve calibration during
 124 training, as they preemptively address miscalibration without relying on post-hoc adjustments. Label
 125 Smoothing (LS) (Szegedy et al., 2016) is one of the foundational techniques, softening the sharp one-
 126 hot label distribution to mitigate overconfidence. Sample-dependent Focal Loss (FLSD) (Mukhoti
 127 et al., 2020) builds upon this by focusing calibration on harder-to-classify examples. Margin-based
 128 Label Smoothing (MbLS) (Liu et al., 2022) selectively smooths predictions based on the margin
 129 between predicted logits and true labels, while Multi-class Difference in Confidence and Accuracy
 130 (MDCA) (Hebbalaguppe et al., 2022) applies this margin adjustment across the entire predicted
 131 distribution. Adaptive and Conditional Label Smoothing (ACLS) (Park et al., 2023) dynamically
 132 adjusts the level of smoothing, applying stronger smoothing to miscalibrated predictions while pre-
 133 serving accurate confidence estimates for well-calibrated ones. While regularization-based calibra-
 134 tion methods have been extensively studied, their application to ordinal tasks remains underexplored,
 135 despite the crucial role of confidence estimation in such settings.

136 3 A UNIFIED LOSS FUNCTIONS FOR CALIBRATION AND UNIMODALITY

137 3.1 LIMITATIONS OF CROSS-ENTROPY IN ORDINAL REGRESSION

138 In ordinal classification tasks, such as medical diagnosis or rating assessments, the inherent order
 139 between classes plays a crucial role. Traditional loss functions, like CE, often fail to capture this
 140 ordinal structure, leading to suboptimal performance and poorly calibrated predictions. This limita-
 141 tion is particularly problematic in high-risk applications where both accurate predictions and reliable
 142 confidence estimates are essential for informed decision-making.

143 Let $y_n \in \{1, \dots, C\}$ denote the true class label of the n -th sample, where N is the total num-
 144 ber of samples and C represents the number of classes. The CE loss is defined as $\mathcal{L}_{\text{CE}} = -\sum_{n=1}^N \sum_{k=1}^C y_{n,k} \log(\hat{y}_{n,k})$ where $y_{n,k}$ is the one-hot encoded true label and $\hat{y}_{n,k}$ is the predicted
 145 probability. The gradient of \mathcal{L}_{CE} with respect to the logit $z_{n,k}$ is: $\frac{\partial \mathcal{L}_{\text{CE}}}{\partial z_{n,k}} = \hat{y}_{n,k} - y_{n,k}$. This formula-
 146 tion forces the model to focus sharply on the true label, often resulting in overconfident predictions
 147 that ignore relationships between adjacent classes. In ordinal tasks, predictions should reflect the
 148 ordered nature of classes, with probability mass distributed smoothly around the true label. How-
 149 ever, \mathcal{L}_{CE} typically produces sharp peaks, disregarding the ordinal structure and potentially leading
 150 to unreliable predictions in critical scenarios.

151 To address these limitations, we propose a novel loss function that explicitly accounts for ordinal
 152 relationships between classes while incorporating a regularization term to enforce unimodality and
 153 improve calibration. Our approach aims to balance accurate ordinal predictions with well-calibrated
 154 confidence estimates, enhancing performance in sensitive applications without compromising over-
 155 all predictive accuracy.

156 3.2 SOFT ORDINAL ENCODING

157 One of the primary limitations of the traditional \mathcal{L}_{CE} loss in ordinal tasks is its reliance on one-hot
 158 encoding, which concentrates probability mass entirely on the true label. This results in overconfi-

162 dent predictions, disregarding the relationships between adjacent classes. To address these issues,
 163 we employ the SORD encoding method (Diaz & Marathe, 2019), which redistributes the probabili-
 164 ty mass across the ordinal classes in a way that reflects both the inherent ordinal structure and the
 165 uncertainty between adjacent labels.

166 In an ordinal classification problem with C classes, the true label y_n for the n -th sample is rep-
 167 resented as a soft-encoded probability distribution $y'_{n,k}$, defined as $y'_{n,k} = \frac{e^{-\phi(y_n, r_k)}}{\sum_{j=1}^C e^{-\phi(y_n, r_j)}}$, for
 168 $k = 1, \dots, C$, where $\phi(y_n, r_k)$ is a distance metric that penalizes deviations from the true class y_n
 169 to each ordinal class r_k during the soft encoding process. The Soft-encoded Cross-Entropy (SCE)
 170 loss is then defined as:

$$172 \quad \mathcal{L}_{\text{SCE}} = - \sum_{n=1}^N \sum_{k=1}^C y'_{n,k} \log(\hat{y}_{n,k}), \quad (1)$$

173 The gradient of \mathcal{L}_{SCE} with respect to the logit $z_{n,k}$ is $\frac{\partial \mathcal{L}_{\text{SCE}}}{\partial z_{n,k}} = \hat{y}_{n,k} - y'_{n,k}$. This gradient encourages
 174 the model to distribute probability across adjacent classes in a way that aligns with the soft-encoded
 175 true label distribution, mitigating overconfidence and resulting in more calibrated predictions that
 176 accurately reflect the ordinal relationships between classes.

177 3.3 ORDER-AWARE REGULARIZATION: ENFORCING UNIMODALITY AND CALIBRATION

178 While \mathcal{L}_{SCE} effectively captures the ordinal relationships between labels and mitigates the overcon-
 179 fidence issue in \mathcal{L}_{CE} , it can still lead to underconfident predictions due to the redistribution of prob-
 180 ability mass across classes. To address this issue, we introduce a regularization-based method that
 181 simultaneously enhances the model’s calibration and reinforces the learning of the ordinal structure
 182 (which inherently leads to unimodality in the output distribution).

183 Unlike traditional regularization methods, which focus solely on the highest probability class and ig-
 184 nore the relationships between adjacent labels (Park et al., 2023), our approach leverages the ordinal
 185 structure of the task. Specifically, our method adjusts the logits based on their ordinal relationship
 186 to the true label y_n , ensuring that the calibration regularization is order-aware. This approach di-
 187 vides the logits into two regions: those where the class index k is smaller than the true label and
 188 those where k is greater than or equal to the true label. By doing so, the regularization ensures
 189 smooth decreases in probability on both sides of the true label, enforcing a unimodal distribution
 190 while simultaneously improving calibration. The specific formulation of the regularization term is
 191 as follows:

$$192 \quad \mathcal{L}_{\text{REG}} = \sum_{n=1}^N \sum_{k=1}^{C-1} \begin{cases} \hat{I}(z_{n,k} - z_{n,k+1}), & \text{if } k < y_n, \\ \hat{I}(z_{n,k+1} - z_{n,k}), & \text{if } k \geq y_n, \end{cases} \quad (2)$$

193 where $\hat{I}(r) = -\frac{1}{t} \log(-r)$ if $r \leq -\frac{1}{t^2}$, and $\hat{I}(r) = tr - \frac{1}{t} \log(\frac{1}{t^2}) + \frac{1}{t}$ otherwise.

194 This penalty function applies strong corrections when the differences between adjacent logits ap-
 195 proach the boundary value $-1/t^2$, ensuring unimodality is preserved. The temperature parameter t
 196 controls the strength of this regularization. The final loss function ORCU, is defined as:

$$197 \quad \mathcal{L}_{\text{ORCU}} = \mathcal{L}_{\text{SCE}} + \mathcal{L}_{\text{REG}}. \quad (3)$$

198 By integrating both \mathcal{L}_{SCE} and \mathcal{L}_{REG} , $\mathcal{L}_{\text{ORCU}}$ ensures that the model produces well-calibrated, uni-
 199 modal predictions that accurately reflect the ordinal relationships between classes.

200 3.4 GRADIENT ANALYSIS: ENFORCING UNIMODALITY AND CALIBRATION

201 The gradient behavior of the proposed regularization term \mathcal{L}_{REG} is crucial for ensuring both uni-
 202 modality and calibration. As illustrated in Figure 1, the $\mathcal{L}_{\text{ORCU}}$ loss applies soft label encoding and
 203 uses regularization differently depending on whether $k < y_n$ or $k \geq y_n$. To better understand its im-
 204 pact, we divide the gradient into four cases based on the relationship between the class index k and
 205 the target label y_n , as well as the magnitude of the difference between adjacent logits r (Table 1-b).
 206 The regularization term adjusts the logits to ensure that the output distribution remains smooth and
 207 unimodal, particularly in ordinal classification tasks.

208 When $k < y_n$ (Figure 1-ii), the model adjusts the logits to ensure that the probability distribution
 209 decreases smoothly as the distance from the true label increases, maintaining a unimodal structure.

Table 1: Gradient analysis of our loss function. The gradient is computed w.r.t. a logit when $k < y_n$ and $k \geq y_n$. We also show the gradient of each term, \mathcal{L}_{SCE} and \mathcal{L}_{REG} , to analyze each one’s contribution. $\hat{y}_{n,k}$ denote the predicted probability, $y'_{n,k}$ representing the soft-encoded target, and t being a variable controlling the regularization strength. Note that $\frac{\partial \mathcal{L}_{\text{ORCU}}}{\partial z_k} = \frac{\partial \mathcal{L}_{\text{SCE}}}{\partial z_k} + \frac{\partial \mathcal{L}_{\text{REG}}}{\partial z_k}$.

	$k < y_n$ ($r = z_{n,k} - z_{n,k+1}$)		$k \geq y_n$ ($r = z_{n,k+1} - z_{n,k}$)	
	$r \leq -\frac{1}{t^2}$	$r > -\frac{1}{t^2}$	$r \leq -\frac{1}{t^2}$	$r > -\frac{1}{t^2}$
(a) $\frac{\partial \mathcal{L}_{\text{SCE}}}{\partial z_{n,k}}$		$\hat{y}_{n,k} - y'_{n,k}$		
(b) $\frac{\partial \mathcal{L}_{\text{REG}}}{\partial z_{n,k}}$	$-\frac{1}{tr}$	t	$\frac{1}{tr}$	$-t$
(c) $\frac{\partial \mathcal{L}_{\text{ORCU}}}{\partial z_{n,k}}$	$\hat{y}_{n,k} - (y'_{n,k} + \frac{1}{tr})$	$\hat{y}_{n,k} - (y'_{n,k} - t)$	$\hat{y}_{n,k} - (y'_{n,k} - \frac{1}{tr})$	$\hat{y}_{n,k} - (y'_{n,k} + t)$

This is achieved by keeping the difference between adjacent logits, r , negative. If r is negative and has a large absolute value, the gradient of \mathcal{L}_{REG} becomes smaller, indicating that the model is close to achieving a unimodal distribution. However, as r approaches the boundary $-\frac{1}{t^2}$, the gradient increases sharply to prevent any violations of unimodality. On the other hand, when $r > -\frac{1}{t^2}$, indicating a deviation from the desired unimodal structure, a constant penalty is applied to restore the distribution.

Dynamic gradient adjustment for simultaneous calibration and unimodality When the gradients of \mathcal{L}_{SCE} and \mathcal{L}_{REG} are combined, the regularization term enables the model to address both calibration and the learning of the ordinal structure (i.e., unimodality) simultaneously.

First, consider the case where $k < y_n$ (as shown in Figure 1-(a-ii)), where the predicted class is lower than the true class. In this scenario, for large positive r values (Figure 1-(b-ii)), the regularization term reduces $y'_{n,k}$ by a factor of t , increasing the difference between $\hat{y}_{n,k}$ and $y'_{n,k} - t$. This larger gradient leads to a more substantial update to the logit z_k , compared to using \mathcal{L}_{SCE} alone. Consequently, this adjustment not only restores unimodality by driving r towards negative values but also helps correct overconfident predictions for incorrect labels. By increasing the gradient for such incorrect predictions, the model is able to reduce the predicted probability for the incorrect class more effectively, improving overall calibration and ordinal structure learning.

Next, consider the case where $k = y_n$, and $r > -\frac{1}{t^2}$ (as shown in Figure 1-(b-iii)). In this underconfident scenario, where the predicted probability $\hat{y}_{n,k}$ is lower than the target distribution $y'_{n,k}$, the regularization term modifies the gradient to $\hat{y}_{n,k} - (y'_{n,k} + t)$. This larger gradient (with a greater absolute value) results in a more substantial update to the logit z_k , increasing the predicted probability for the true class y_n . At the same time, this adjustment restores unimodality by ensuring that r remains negative, aligning the probability distribution smoothly around the true label.

By combining these two examples, we demonstrate that the proposed \mathcal{L}_{REG} term dynamically adjusts the gradients based on the value of r , enabling the model to simultaneously achieve well-calibrated predictions and maintain the ordinal structure (unimodality) of the task. Whether the model is overconfident or underconfident, the regularization term ensures appropriate updates to the logits, balancing both calibration and the preservation of the ordinal relationships between classes. This dual mechanism is essential for high-risk ordinal tasks, where both accurate predictions and reliable confidence estimates are critical.

4 EXPERIMENTS

4.1 DATASETS AND IMPLEMENTATION DETAILS

We evaluated the proposed $\mathcal{L}_{\text{ORCU}}$ loss function on three public datasets selected for their ordinal nature and sufficient sample sizes, covering diverse tasks such as age estimation, image aesthetics assessment, and medical diagnosis. The Adience dataset (Eidinger et al., 2014), containing 26,580 images categorized into 8 age groups, was used for age estimation, employing five-fold cross-validation

with an 80/20 train-test split¹. For image aesthetics assessment, the Image Aesthetics dataset (Schifanella et al., 2015), consisting of 13,364 images with five ordinal labels, was used with five-fold cross-validation and an 80/20 train-test split. The LIMUC dataset (Polat et al., 2022a), comprising 11,276 images from ulcerative colitis patients with four mayo endoscopic scores (MES), was used for medical diagnosis, employing an 85/15 subject-exclusive (Paplhám et al., 2024) train-test split and a ten-fold cross-validation protocol (Polat et al., 2022b).

For all tasks, we used a ResNet-50 architecture (He et al., 2015) pretrained on ImageNet (Russakovsky et al., 2015). We applied a layer-wise learning rate strategy (0.01 for the fully connected layer, 0.001 for others), using AdamW (Loshchilov & Hutter, 2019) for optimization. Training was conducted for 100 epochs with a batch size of 64, applying image augmentations via Albumentations (Buslaev et al., 2020). The squared distance metric was used for soft encoding, with the temperature parameter t initialized at 10.0 and gradually decreased throughout training. All experiments were conducted on NVIDIA RTX 4090 GPUs.

4.2 PERFORMANCE METRICS

Evaluating calibration is crucial in ordinal classification tasks, where models must provide not only accurate predictions but also reliable confidence estimates. We focus on two specific calibration metrics: static calibration error (SCE) and adaptive calibration error (ACE)², which are particularly suited to addressing class imbalances and capturing calibration across all predictions. Although expected calibration error (ECE) is commonly used, it can be misleading, especially in imbalanced datasets where confidence is skewed towards high-probability predictions, failing to accurately reflect model performance in all classes (Nixon et al., 2019). SCE and ACE provide more robust measures of calibration by evaluating calibration per class or dynamically adjusting bin sizes.

To capture ordinal relationships between classes, we use quadratic weighted kappa (QWK) as the primary metric, as it penalizes larger misclassifications more heavily and better reflects the distance between predicted and true labels compared to accuracy. Although accuracy is reported, QWK serves as the primary metric for assessing classification performance in ordinal tasks.

4.3 RESULTS AND ANALYSIS

Our proposed loss function $\mathcal{L}_{\text{ORCU}}$ demonstrates superior performance across both calibration and ordinal regression metrics, surpassing baseline methods designed for either objective individually (Table 2). Unlike existing loss functions that primarily focus on a single goal—either calibration or classification— $\mathcal{L}_{\text{ORCU}}$ effectively balances both, achieving significant improvements in calibration metrics while maintaining strong predictive accuracy.

In high-stakes tasks such as medical diagnosis and severity grading, where accurate and well-calibrated predictions are critical, $\mathcal{L}_{\text{ORCU}}$ proves particularly advantageous. Existing ordinal loss functions, such as CE and its variants, tend to overlook calibration error, while traditional calibration losses fail to account for the ordinal structure that is intrinsic to these tasks. To thoroughly evaluate $\mathcal{L}_{\text{ORCU}}$, we compared it against 10 baseline loss functions, categorized into two groups: ordinal loss functions—CE, SORD (Diaz & Marathe, 2019), CDW-CE (Polat et al., 2022b), CO2 (Albuquerque et al., 2021), and POE (Li et al., 2021)—and calibration loss functions—LS (Szegedy et al., 2016), FLSD (Mukhoti et al., 2020), MbLS (Liu et al., 2022), MDCA (Hebbalaguppe et al., 2022), and ACLS (Park et al., 2023). Each loss function was evaluated under identical experimental conditions to ensure fair benchmarking.

4.3.1 COMPARISON WITH LOSS FUNCTIONS TARGETING INDIVIDUAL OBJECTIVES

Comparison with Ordinal Loss Functions Our method, $\mathcal{L}_{\text{ORCU}}$, consistently outperforms all baseline ordinal loss functions, providing superior calibration and classification performance. As detailed in Table 2, $\mathcal{L}_{\text{ORCU}}$ achieves the lowest SCE, ACE, and ECE scores, while maintaining competitive accuracy and QWK scores. This highlights its ability to deliver well-calibrated predictions without compromising on predictive performance. Traditional ordinal loss function, primarily focus

¹<https://github.com/GilLevi/AgeGenderDeepLearning>

²https://github.com/Jonathan-Pearce/calibration_library

324
 325 Table 2: Calibration and accuracy performance for different loss functions on three popular ordinal
 326 regression benchmarks. Competing methods in two areas, i.e., ordinal regression and network cali-
 327 bration, are compared with ours. We use ResNet-50 for classifications and use 15 bins for calibration
 328 metrics calculation. The measures are presented as the mean and standard deviation over all folds.

Loss	Evaluation Metrics				
	SCE(\downarrow)	ACE(\downarrow)	ECE(\downarrow)	Acc(\uparrow)	QWK(\uparrow)
Adience ($n = 17,423$)					
Ordinal Loss	Cross Entropy	0.8495 \pm 0.0033	0.8356 \pm 0.0068	0.3364 \pm 0.0401	0.5639 \pm 0.0486
	SORD (Diaz & Marathe, 2019)	0.7823 \pm 0.0105	0.7783 \pm 0.0102	0.0731 \pm 0.0240	0.5910 \pm 0.0439
	CDW-CE (Polat et al., 2022b)	0.8429 \pm 0.0062	0.8372 \pm 0.0071	0.2913 \pm 0.0210	0.5789 \pm 0.0362
	CO2 (Albuquerque et al., 2021)	0.8521 \pm 0.0055	0.8368 \pm 0.0080	0.3533 \pm 0.0406	0.5637 \pm 0.0489
	POE (Li et al., 2021)	0.8340 \pm 0.0042	0.8244 \pm 0.0065	0.2733 \pm 0.0384	0.5652 \pm 0.0522
Calibration Loss	LS (Szegedy et al., 2016)	0.8195 \pm 0.0071	0.8101 \pm 0.0072	0.1890 \pm 0.0415	0.5792 \pm 0.0495
	FLSD (Mukhoti et al., 2020)	0.8474 \pm 0.0063	0.8340 \pm 0.0062	0.3193 \pm 0.0407	0.5718 \pm 0.0532
	MbLS (Liu et al., 2022)	0.8400 \pm 0.0043	0.8323 \pm 0.0052	0.2815 \pm 0.0344	0.5765 \pm 0.0489
	MDCA(Hebbalaguppe et al., 2022)	0.8561 \pm 0.0527	0.8365 \pm 0.0059	0.3372 \pm 0.0411	0.5676 \pm 0.0488
	ACLS (Park et al., 2023)	0.8398 \pm 0.0040	0.8295 \pm 0.0045	0.2847 \pm 0.0378	0.5762 \pm 0.0488
ORCU (Ours)		0.4598 \pm 0.0435	0.4565 \pm 0.0437	0.0583 \pm 0.0279	0.5878 \pm 0.0426
Image Aesthetics ($n = 13,364$)					
Ordinal Loss	Cross Entropy	0.7637 \pm 0.0037	0.7558 \pm 0.0035	0.2057 \pm 0.0162	0.7030 \pm 0.0080
	SORD (Diaz & Marathe, 2019)	0.6844 \pm 0.0018	0.6833 \pm 0.0018	0.1846 \pm 0.0026	0.7092 \pm 0.0044
	CDW-CE (Polat et al., 2022b)	0.7519 \pm 0.0030	0.7480 \pm 0.0026	0.1751 \pm 0.0136	0.7041 \pm 0.0064
	CO2 (Albuquerque et al., 2021)	0.7699 \pm 0.0032	0.7614 \pm 0.0036	0.2269 \pm 0.0151	0.6980 \pm 0.0072
	POE (Li et al., 2021)	0.7559 \pm 0.0020	0.7493 \pm 0.0035	0.1883 \pm 0.0111	0.7010 \pm 0.0097
Calibration Loss	LS (Szegedy et al., 2016)	0.7222 \pm 0.0010	0.7179 \pm 0.0014	0.0991 \pm 0.0062	0.7063 \pm 0.0054
	FLSD (Mukhoti et al., 2020)	0.7519 \pm 0.0030	0.7482 \pm 0.0026	0.1751 \pm 0.0136	0.7013 \pm 0.0075
	MbLS (Liu et al., 2022)	0.7577 \pm 0.0016	0.7510 \pm 0.0020	0.1895 \pm 0.0062	0.7040 \pm 0.0057
	MDCA(Hebbalaguppe et al., 2022)	0.7620 \pm 0.0033	0.7549 \pm 0.0033	0.2022 \pm 0.0124	0.7031 \pm 0.0110
	ACLS (Park et al., 2023)	0.7595 \pm 0.0010	0.7535 \pm 0.0013	0.1957 \pm 0.0097	0.7030 \pm 0.0091
ORCU (Ours)		0.6805 \pm 0.0045	0.6794 \pm 0.0046	0.1082 \pm 0.0312	0.7113 \pm 0.0038
LIMUC ($n = 11,276$)					
Ordinal Loss	Cross Entropy	0.6997 \pm 0.0076	0.6948 \pm 0.0075	0.1295 \pm 0.0170	0.7702 \pm 0.0066
	SORD (Diaz & Marathe, 2019)	0.6382 \pm 0.0031	0.6370 \pm 0.0032	0.1636 \pm 0.0064	0.7749 \pm 0.0060
	CDW-CE (Polat et al., 2022b)	0.6980 \pm 0.0048	0.6927 \pm 0.0042	0.1190 \pm 0.0096	0.7773 \pm 0.0058
	CO2 (Albuquerque et al., 2021)	0.7105 \pm 0.0044	0.7042 \pm 0.0042	0.1544 \pm 0.0118	0.7662 \pm 0.0076
	POE (Li et al., 2021)	0.6933 \pm 0.0043	0.6881 \pm 0.0046	0.1149 \pm 0.0105	0.7724 \pm 0.0040
Calibration Loss	LS (Szegedy et al., 2016)	0.6647 \pm 0.0010	0.6603 \pm 0.0022	0.0592 \pm 0.0088	0.7633 \pm 0.0053
	FLSD (Mukhoti et al., 2020)	0.6674 \pm 0.0016	0.6631 \pm 0.0022	0.1069 \pm 0.0167	0.7657 \pm 0.0059
	MbLS (Liu et al., 2022)	0.6988 \pm 0.0022	0.6982 \pm 0.0035	0.1301 \pm 0.0095	0.7665 \pm 0.0057
	MDCA(Hebbalaguppe et al., 2022)	0.6934 \pm 0.0074	0.6879 \pm 0.0061	0.1197 \pm 0.0129	0.7683 \pm 0.0044
	ACLS (Park et al., 2023)	0.6995 \pm 0.0030	0.6939 \pm 0.0032	0.1299 \pm 0.0140	0.7683 \pm 0.0064
ORCU (Ours)		0.5205 \pm 0.0098	0.5182 \pm 0.0107	0.0853 \pm 0.0269	0.7785 \pm 0.0064

364
 365 on accuracy but tend to produce overconfident predictions by concentrating probability mass on the
 366 true label (Figure 2-a, c-e). Although SORD reduces overconfidence by distributing probability
 367 mass across adjacent labels, it results in underconfident predictions (Figure 2-c), limiting its effec-
 368 tiveness. In contrast, $\mathcal{L}_{\text{ORCU}}$ effectively balances these extremes. As shown in Figure 2-f, our method
 369 mitigates both overconfidence and underconfidence, delivering well-calibrated confidence estimates.
 370 Additionally, high QWK scores across all datasets confirm that $\mathcal{L}_{\text{ORCU}}$ captures the inherent ordinal
 371 relationships between classes more effectively than baseline ordinal loss functions.

372 **Comparison with Calibration Loss Functions** When compared with calibration-focused loss
 373 functions, $\mathcal{L}_{\text{ORCU}}$ also demonstrates superior performance. Calibration losses like LS, FLSD, MbLS,
 374 MDCA, and ACLS are primarily designed to reduce calibration error in nominal tasks, without
 375 considering the ordinal relationships between classes. However, $\mathcal{L}_{\text{ORCU}}$ incorporates these ordinal
 376 relationships into the calibration process, which leads to superior results in tasks that require both
 377 accurate predictions and well-calibrated confidence estimates. As seen in Table 2, $\mathcal{L}_{\text{ORCU}}$ consis-
 378 tently achieves the lowest SCE and ACE scores, while also delivering strong accuracy and QWK
 379 scores. Although LS slightly outperforms $\mathcal{L}_{\text{ORCU}}$ in ECE, it fails to account for the ordinal struc-

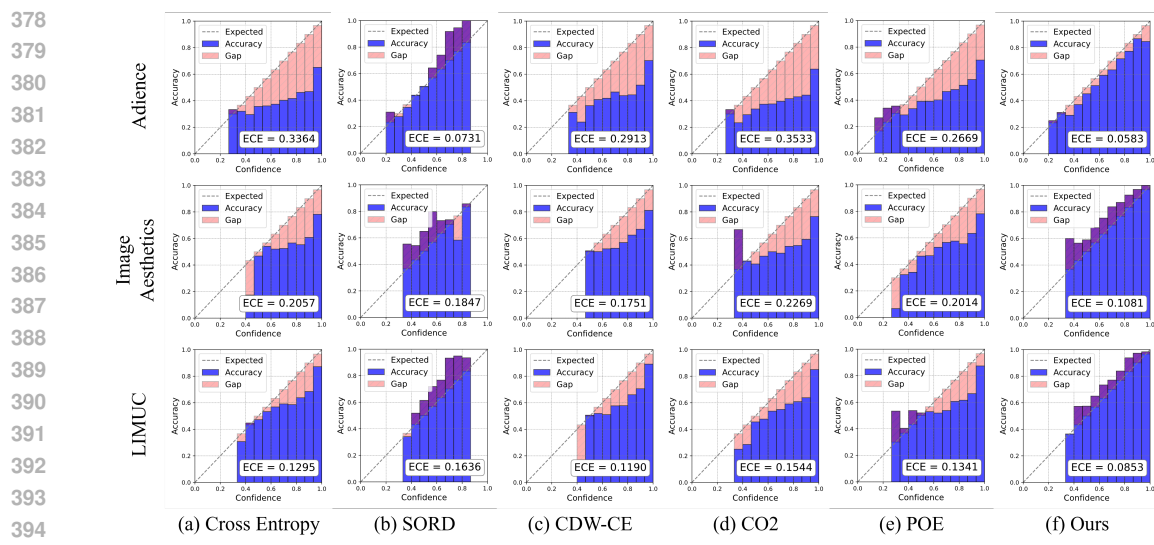


Figure 2: Reliability diagrams for different ordinal loss functions. The diagrams show model confidence alongside the calibration gap between confidence and accuracy, using the test split of Adience, Image Aesthetics, and LIMUC. Predictions above the diagonal, expected line indicate underconfidence, while those below the line represent overconfidence. ECE is computed using 15 bins.

ture, as evidenced by its lower QWK scores. This demonstrates the advantage of $\mathcal{L}_{\text{ORCU}}$ in ordinal classification tasks, where preserving the relationships between labels is critical.

In summary, $\mathcal{L}_{\text{ORCU}}$ provides a balanced solution for both calibration and classification, outperforming loss functions designed for either objective individually. By delivering well-calibrated predictions while maintaining high accuracy and QWK scores, $\mathcal{L}_{\text{ORCU}}$ effectively addresses the dual challenges of calibration and ordinal classification. This makes it particularly valuable in such critical tasks where both aspects are essential.

Table 3: Ablation study on different distance metrics used in the soft encoding. The table analyzes the performance impact of applying various distance metrics (absolute, Huber, exponential, and squared) across multiple datasets. The results are presented as the mean and standard deviation over all folds.

Evaluation Metrics	SCE(\downarrow)	ACE(\downarrow)	ECE(\downarrow)	Acc(\uparrow)	QWK(\uparrow)
Distance Metrics ϕ					
Adience ($n = 17,423$)					
Absolute	0.7121 ± 0.0088	0.7167 ± 0.0088	0.0684 ± 0.0203	0.5800 ± 0.0334	0.8961 ± 0.0299
Huber	0.7274 ± 0.0110	0.7233 ± 0.0115	0.0553 ± 0.0084	0.5704 ± 0.0461	0.8948 ± 0.0323
Exponential	0.7774 ± 0.0120	0.7753 ± 0.0116	0.0868 ± 0.0262	0.5794 ± 0.0425	0.8983 ± 0.0320
Squared	0.4598 ± 0.0435	0.4565 ± 0.0437	0.0583 ± 0.0279	0.5878 ± 0.0426	0.9036 ± 0.0281
Image Aesthetics ($n = 13,364$)					
Absolute	0.6849 ± 0.0020	0.6837 ± 0.0018	0.1351 ± 0.0153	0.7101 ± 0.0044	0.5175 ± 0.0117
Huber	0.6827 ± 0.0016	0.6839 ± 0.0034	0.1460 ± 0.0180	0.7077 ± 0.0083	0.5127 ± 0.0167
Exponential	0.6869 ± 0.0016	0.6859 ± 0.0014	0.1798 ± 0.0052	0.7156 ± 0.0036	0.5265 ± 0.0125
Squared	0.6805 ± 0.0045	0.6794 ± 0.0046	0.1082 ± 0.0312	0.7113 ± 0.0038	0.5188 ± 0.0139
LIMUC ($n = 11,276$)					
Absolute	0.6414 ± 0.0010	0.6406 ± 0.0011	0.1552 ± 0.0113	0.7824 ± 0.0021	0.8625 ± 0.0033
Huber	0.6405 ± 0.0037	0.6399 ± 0.0038	0.1914 ± 0.0136	0.7809 ± 0.0075	0.8599 ± 0.0059
Exponential	0.6397 ± 0.0036	0.6391 ± 0.0036	0.2286 ± 0.0150	0.7794 ± 0.0072	0.8586 ± 0.0055
Squared	0.5205 ± 0.0098	0.5182 ± 0.0107	0.0853 ± 0.0269	0.7785 ± 0.0064	0.8578 ± 0.0048

4.3.2 ABLATION STUDIES

Impact of distance metrics on calibration and prediction The choice of distance metric in soft encoding is a key factor affecting both calibration and prediction performance. Given our focus on

432
 433 Table 4: Ablation study showing impacts of different calibration regularization methods in soft
 434 label encoding. Our method is compared with $\mathcal{L}_{\text{MbLS}}$, $\mathcal{L}_{\text{MDCA}}$, and $\mathcal{L}_{\text{ACLS}}$. The results demonstrate
 435 the importance of incorporating order-aware conditions in the regularization term, which leads to
 436 improved calibration.

Evaluation Metrics Combination	SCE(\downarrow)	ACE(\downarrow)	ECE(\downarrow)	Acc(\uparrow)	QWK(\uparrow)
Adience ($n = 17,423$)					
$\mathcal{L}_{\text{SCE}} + \mathcal{L}_{\text{MbLS_REG}}$	0.7823 ± 0.0092	0.7788 ± 0.0092	0.0711 ± 0.0217	0.5906 ± 0.0418	0.8988 ± 0.0298
$\mathcal{L}_{\text{SCE}} + \mathcal{L}_{\text{MDCA_REG}}$	0.7849 ± 0.0091	0.7810 ± 0.0100	0.0677 ± 0.0315	0.5975 ± 0.0470	0.9024 ± 0.0289
$\mathcal{L}_{\text{SCE}} + \mathcal{L}_{\text{ACLS_REG}}$	0.7827 ± 0.0099	0.7791 ± 0.0100	0.0746 ± 0.0239	0.5936 ± 0.0453	0.9000 ± 0.0322
$\mathcal{L}_{\text{SCE}} + \mathcal{L}_{\text{ORCU_REG}} \text{ (Ours)}$	0.4598 ± 0.0435	0.4565 ± 0.0437	0.0583 ± 0.0279	0.5878 ± 0.0426	0.9036 ± 0.0281
Image Aesthetics ($n = 13,364$)					
$\mathcal{L}_{\text{SCE}} + \mathcal{L}_{\text{MbLS_REG}}$	0.6866 ± 0.0021	0.6852 ± 0.0023	0.1921 ± 0.0057	0.7140 ± 0.0057	0.5106 ± 0.0116
$\mathcal{L}_{\text{SCE}} + \mathcal{L}_{\text{MDCA_REG}}$	0.6867 ± 0.0033	0.6859 ± 0.0035	0.1501 ± 0.0080	0.7156 ± 0.0088	0.4960 ± 0.0192
$\mathcal{L}_{\text{SCE}} + \mathcal{L}_{\text{ACLS_REG}}$	0.6836 ± 0.0028	0.6819 ± 0.0033	0.1829 ± 0.0081	0.7058 ± 0.0082	0.5033 ± 0.0130
$\mathcal{L}_{\text{SCE}} + \mathcal{L}_{\text{ORCU_REG}} \text{ (Ours)}$	0.6805 ± 0.0045	0.6794 ± 0.0046	0.1082 ± 0.0312	0.7113 ± 0.0038	0.5188 ± 0.0139
LIMUC ($n = 11,276$)					
$\mathcal{L}_{\text{SCE}} + \mathcal{L}_{\text{MbLS_REG}}$	0.6398 ± 0.0026	0.6386 ± 0.0026	0.1662 ± 0.0056	0.7784 ± 0.0051	0.8564 ± 0.0035
$\mathcal{L}_{\text{SCE}} + \mathcal{L}_{\text{MDCA_REG}}$	0.6387 ± 0.0026	0.6368 ± 0.0027	0.1373 ± 0.0065	0.7725 ± 0.0056	0.8544 ± 0.0043
$\mathcal{L}_{\text{SCE}} + \mathcal{L}_{\text{ACLS_REG}}$	0.6366 ± 0.0029	0.6349 ± 0.0030	0.1590 ± 0.0067	0.7710 ± 0.0061	0.8532 ± 0.0052
$\mathcal{L}_{\text{SCE}} + \mathcal{L}_{\text{ORCU_REG}} \text{ (Ours)}$	0.5205 ± 0.0098	0.5182 ± 0.0107	0.0853 ± 0.0269	0.7785 ± 0.0064	0.8578 ± 0.0048

451
 452 achieving reliable, well-calibrated predictions in high-risks ordinal regression tasks, we compared
 453 four common distance metrics: Absolute, Squared, Huber, and Exponential. As shown in Table 3,
 454 the Squared distance metric consistently provided the best calibration results, particularly in terms
 455 of ECE, ACE, and SCE. While Absolute and Exponential metrics showed competitive classification
 456 performance on some datasets, they delivered less reliable calibration, making them less suitable for
 457 high-risk tasks. In contrast, the Squared metric offered a balanced improvement in both calibration
 458 and prediction accuracy, making it the most effective choice for our loss function.

459 **Importance of order-aware regularization method** We conducted an ablation study to assess
 460 the effect of different calibration regularization methods applied within the \mathcal{L}_{SCE} . Our approach,
 461 which integrates both calibration and unimodality constraints, demonstrated consistently superior
 462 calibration results, lower SCE, ACE, and ECE scores (see Table 4). Unlike traditional methods that
 463 focus calibration only on the highest probability class and overlook ordinal relationships, our method
 464 applies calibration across all labels, ensuring the entire ordinal structure is respected. This approach
 465 led to improved calibration metrics (SCE, ACE, ECE) and higher QWK scores, which better capture
 466 the model’s ability to reflect the inherent order of labels. Although there was a slight decrease in
 467 accuracy, this minimal trade-off is offset by the significant gains in calibration and QWK, making it
 468 particularly valuable for high-risk, ordinal classification tasks.
 469

5 CONCLUSION

470 We introduced ORCU, a unified loss function that integrates calibration and unimodality for ordinal
 471 regression. Calibration has been overlooked in the literature on ordinal tasks, despite its importance
 472 in high-risk applications. ORCU addresses the issue by explicitly targeting calibration improvement
 473 in ordinal regression, using comprehensive metrics such as SCE, ACE and ECE to evaluate its effec-
 474 tiveness. By leveraging soft ordinal encoding and order-aware regularization, which simultaneously
 475 enforces calibration and unimodality, ORCU balances accurate predictions with well-calibrated con-
 476 fidence estiamtes. Without requiring any architectural changes, our method consistently outper-
 477 formed the latest loss functions in the domains of calibration and ordinal regression. This work sets
 478 a new benchmark for reliable ordinal classification and points the way for future research to optimize
 479 regularization parameter t and extend the approach to more diverse and larger datasets, fostering the
 480 deployment of more robust calibration methods for a wider range of tasks.
 481

REFERENCES

- 482 Tomé Albuquerque, Ricardo Cruz, and Jaime S Cardoso. Ordinal losses for classification of cervical
 483 cancer risk. *PeerJ Computer Science*, 7:e457, 2021.

- 486 Alexander Buslaev, Vladimir I. Iglovikov, Eugene Khvedchenya, Alex Parinov, Mikhail Druzhinin,
 487 and Alexandr A. Kalinin. Albumentations: Fast and flexible image augmentations. *Information*,
 488 11(2):125, February 2020. ISSN 2078-2489. doi: 10.3390/info11020125. URL <http://dx.doi.org/10.3390/info11020125>.
- 489
- 490 Wenzhi Cao, Vahid Mirjalili, and Sebastian Raschka. Rank consistent ordinal regression for neural
 491 networks with application to age estimation. *Pattern Recognition Letters*, 140:325–331, 2020.
- 492
- 493 Shixing Chen, Caojin Zhang, Ming Dong, Jialiang Le, and Mike Rao. Using ranking-cnn for age
 494 estimation. In *Proceedings of the IEEE conference on computer vision and pattern recognition*,
 495 pp. 5183–5192, 2017.
- 496
- 497 Raul Diaz and Amit Marathe. Soft labels for ordinal regression. In *Proceedings of the IEEE/CVF
 498 conference on computer vision and pattern recognition*, pp. 4738–4747, 2019.
- 499
- 500 Eran Eidinger, Roee Enbar, and Tal Hassner. Age and gender estimation of unfiltered faces. *IEEE
 501 Transactions on information forensics and security*, 9(12):2170–2179, 2014.
- 502
- 503 Yun Fu and Thomas S Huang. Human age estimation with regression on discriminative aging man-
 504 ifold. *IEEE Transactions on Multimedia*, 10(4):578–584, 2008.
- 505
- 506 Chuan Guo, Geoff Pleiss, Yu Sun, and Kilian Q Weinberger. On calibration of modern neural
 507 networks. In *International conference on machine learning*, pp. 1321–1330. PMLR, 2017.
- 508
- 509 Kaiming He, Xiangyu Zhang, Shaoqing Ren, and Jian Sun. Deep residual learning for image recog-
 510 nition, 2015. URL <https://arxiv.org/abs/1512.03385>.
- 511
- 512 Ramya Hebbalaguppe, Jatin Prakash, Neelabh Madan, and Chetan Arora. A stitch in time saves
 513 nine: A train-time regularizing loss for improved neural network calibration. In *Proceedings of
 514 the IEEE/CVF Conference on Computer Vision and Pattern Recognition*, pp. 16081–16090, 2022.
- 515
- 516 Qiang Li, Jingjing Wang, Zhaoliang Yao, Yachun Li, Pengju Yang, Jingwei Yan, Chunmao Wang,
 517 and Shiliang Pu. Unimodal-concentrated loss: Fully adaptive label distribution learning for or-
 518 dinal regression. In *Proceedings of the IEEE/CVF Conference on Computer Vision and Pattern
 519 Recognition*, pp. 20513–20522, 2022.
- 520
- 521 Wanhua Li, Jiwen Lu, Jianjiang Feng, Chunjing Xu, Jie Zhou, and Qi Tian. Bridgenet: A continuity-
 522 aware probabilistic network for age estimation. In *Proceedings of the IEEE/CVF conference on
 523 computer vision and pattern recognition*, pp. 1145–1154, 2019.
- 524
- 525 Wanhua Li, Xiaoke Huang, Jiwen Lu, Jianjiang Feng, and Jie Zhou. Learning probabilistic ordinal
 526 embeddings for uncertainty-aware regression. In *Proceedings of the IEEE/CVF conference on
 527 computer vision and pattern recognition*, pp. 13896–13905, 2021.
- 528
- 529 Bingyuan Liu, Ismail Ben Ayed, Adrian Galdran, and Jose Dolz. The devil is in the margin: Margin-
 530 based label smoothing for network calibration. In *Proceedings of the IEEE/CVF Conference on
 531 Computer Vision and Pattern Recognition*, pp. 80–88, 2022.
- 532
- 533 Xiaofeng Liu, Fangfang Fan, Lingsheng Kong, Zhihui Diao, Wanqing Xie, Jun Lu, and Jane You.
 534 Unimodal regularized neuron stick-breaking for ordinal classification. *Neurocomputing*, 388:34–
 535 44, 2020.
- 536
- 537 Ilya Loshchilov and Frank Hutter. Decoupled weight decay regularization, 2019. URL <https://arxiv.org/abs/1711.05101>.
- 538
- 539 Jooyoung Moon, Jihyo Kim, Younghak Shin, and Sangheum Hwang. Confidence-aware learning for
 540 deep neural networks. In *international conference on machine learning*, pp. 7034–7044. PMLR,
 2020.
- 541
- 542 Jishnu Mukhoti, Viveka Kulharia, Amartya Sanyal, Stuart Golodetz, Philip Torr, and Puneet Dokra-
 543 nia. Calibrating deep neural networks using focal loss. *Advances in Neural Information Process-
 544 ing Systems*, 33:15288–15299, 2020.

- 540 Lukas Neumann, Andrew Zisserman, and Andrea Vedaldi. Relaxed softmax: Efficient confidence
 541 auto-calibration for safe pedestrian detection. 2018.
- 542
- 543 Zhenxing Niu, Mo Zhou, Le Wang, Xinbo Gao, and Gang Hua. Ordinal regression with multiple
 544 output cnn for age estimation. In *Proceedings of the IEEE Conference on Computer Vision and*
 545 *Pattern Recognition (CVPR)*, June 2016.
- 546 Jeremy Nixon, Michael W Dusenberry, Linchuan Zhang, Ghassen Jerfel, and Dustin Tran. Measur-
 547 ing calibration in deep learning. In *CVPR workshops*, volume 2, 2019.
- 548
- 549 Hongyu Pan, Hu Han, Shiguang Shan, and Xilin Chen. Mean-variance loss for deep age estimation
 550 from a face. In *Proceedings of the IEEE conference on computer vision and pattern recognition*,
 551 pp. 5285–5294, 2018.
- 552 Jakub Paplham, Vojt Franc, et al. A call to reflect on evaluation practices for age estimation: Com-
 553 parative analysis of the state-of-the-art and a unified benchmark. In *Proceedings of the IEEE/CVF*
 554 *Conference on Computer Vision and Pattern Recognition*, pp. 1196–1205, 2024.
- 555
- 556 Hyekang Park, Jongyoun Noh, Youngmin Oh, Donghyeon Baek, and Bumsub Ham. Acls: Adap-
 557 tive and conditional label smoothing for network calibration. In *Proceedings of the IEEE/CVF*
 558 *International Conference on Computer Vision*, pp. 3936–3945, 2023.
- 559 G Polat, HT Kani, I Ergenc, YO Alahdab, A Temizel, and O Atug. Labeled images for ulcerative
 560 colitis (limuc) dataset. Accessed March, 2022a.
- 561
- 562 Gorkem Polat, Ilkay Ergenc, Haluk Tarik Kani, Yesim Ozen Alahdab, Ozlen Atug, and Alptekin
 563 Temizel. Class distance weighted cross-entropy loss for ulcerative colitis severity estimation.
 564 In *Annual Conference on Medical Image Understanding and Analysis*, pp. 157–171. Springer,
 2022b.
- 565
- 566 Olga Russakovsky, Jia Deng, Hao Su, Jonathan Krause, Sanjeev Satheesh, Sean Ma, Zhiheng
 567 Huang, Andrej Karpathy, Aditya Khosla, Michael Bernstein, et al. Imagenet large scale visual
 568 recognition challenge. *International journal of computer vision*, 115:211–252, 2015.
- 569 Rossano Schifanella, Miriam Redi, and Luca Maria Aiello. An image is worth more than a thousand
 570 favorites: Surfacing the hidden beauty of flickr pictures. In *Proceedings of the international AAAI*
 571 *conference on web and social media*, volume 9, pp. 397–406, 2015.
- 572
- 573 Xintong Shi, Wenzhi Cao, and Sebastian Raschka. Deep neural networks for rank-consistent ordinal
 574 regression based on conditional probabilities. *Pattern Analysis and Applications*, 26(3):941–955,
 2023.
- 575
- 576 Christian Szegedy, Vincent Vanhoucke, Sergey Ioffe, Jon Shlens, and Zbigniew Wojna. Rethink-
 577 ing the inception architecture for computer vision. In *Proceedings of the IEEE conference on*
 578 *computer vision and pattern recognition*, pp. 2818–2826, 2016.
- 579
- 580 Vctor Manuel Vargas, Pedro Antonio Gutirrez, and Cesar Hervs-Martnez. Unimodal regulari-
 581 sation based on beta distribution for deep ordinal regression. *Pattern Recognition*, 122:108310,
 2022.
- 582
- 583 Tsun-Yi Yang, Yi-Hsuan Huang, Yen-Yu Lin, Pi-Cheng Hsiu, and Yung-Yu Chuang. Ssr-net: A
 584 compact soft stagewise regression network for age estimation. In *IJCAI*, volume 5, pp. 7, 2018.
- 585
- 586
- 587 **A APPENDIX**
- 588
- 589 You may include other additional sections here.
- 590
- 591
- 592
- 593